JOURNAL OF COMPUTATIONAL PHYSICS 78, 437–458 (1988)

Assessment of Riemann Solvers for Unsteady One-Dimensional Inviscid Flows of Perfect Gases

J. J. GOTTLIEB AND C. P. T. GROTH

Institute for Aerospace Studies, University of Toronto
4925 Dufferin Street, Downsview, Ontario, Canada M3H5T6

Received June 8, 1987

The solution of Riemann problems for the one-dimensional Euler equations with polytropic gases usually involves a numerical iterative solution procedure, and more efficient Riemann solvers can reduce computational times and costs by factors of up to 25. Riemann solvers that have been used in past computational fluid dynamics, those that are used in current numerical work, and a new and more efficient one reported in this paper are all assessed in terms of their relative computational performance. This assessment includes the type of shock and rarefaction-wave equations, iterative procedures, and initial guesses used by Godunov, Chorin, Van Leer, Smoller, and others. Various aspects of the Riemann problem and its solution for unsteady flows are also discussed in terms of the pressure-velocity diagram, both for completeness and to add some new practical insights for improving computer codes.

1. INTRODUCTION

Riemann problems and related solution procedures were first introduced into computational fluid dynamics by Godunov [1–3], in his special finite-difference methods for solving one- and two-dimensional unsteady inviscid gas flows. Glimm [4] later employed Riemann problems in conjunction with a new random sampling procedure as a theoretical tool to derive existence proofs for all time for weak solutions of hyperbolic systems of conservation laws. The existence and uniqueness of solutions for general Riemann problems with arbitrary initial data has been the subject of intensive study (e.g., see [5–7]).

The initial study of Glimm [4] and later work by Moler and Smoller [8] stimulated Chorin [9, 10] to make Glimm's method into a practical computational tool for solving problems in gas dynamics. Various improvements to Glimm's method were subsequently made by others such as Sod [11], Roe [12], Colella [13], Colella and Glaz [14], and Gottlieb [15], and this technique is now well known as the random-choice method (RCM). The RCM makes extensive use of Riemann solvers and has been used successfully to solve a number of practical problems in gas dynamics [11, 16–20], underwater explosions [21, 22], and special problems related to two-phase flow of petroleum in underground reservoirs [23].

0021-9991/88 $3.00

The increased usage of Riemann solvers in various numerical solution schemes of computational fluid dynamics has stimulated the demand for more efficient iterative solution procedures, in order to reduce the often excessive computational times and costs. Although some previous work has been done on approximate Riemann solvers [1–3, 12, 14], this study presents an assessment of the relative performance of a collection of exact Riemann solvers which are appropriate for solving one- and two-dimensional unsteady flows of thermally and calorically perfect gases (polytropic). Furthermore, a new and more efficient solver is given and also assessed. These results should help researchers and engineers choose a suitable Riemann solver for their computer codes.

An introduction to the Riemann problem for the specific case of unsteady one-dimensional flows of perfect gases is presented in Section 2, including a description of its solution based on the pressure–velocity diagram. This is a prerequisite to the presentation of the different Riemann solvers appearing in Section 3 and the assessment of these solvers which follows in Section 4.

2. Riemann Problem

For one-dimensional nonstationary flows the state U of a perfect gas is specified completely by three dependent variables and two constants that are particular to the type of gas. Three convenient dependent variables are the pressure p, density ρ, and flow velocity u, and two fairly convenient constants are the ratio of the specific heats γ and gas constant R. From these variables and constants all of the other state properties may be obtained. For example, the temperature T may be obtained from the equation of state ($p=\rho RT$) and the sound speed a follows from its definition ($a^2=\gamma RT=\gamma p/\rho$). Hence, the state U may be completely defined by (p, ρ, u, γ, R), or alternately (p, a, u, γ, R).

Now consider two discrete initial states $U(x_i, t_j)$ and $U(x_{i+1}, t_j)$ at adjacent nodes at time level t_j of the discretized numerical grid depicted in Fig. 1. The initial value or Riemann problem may then be expressed as

$$U(x, t_j)=\begin{cases} U(x_i, t_j) & \text{if} \quad x < x_i+\Omega(x_i-x_{i+1}), \\ U(x_{i+1}, t_j) & \text{if} \quad x \geqslant x_i+\Omega(x_i-x_{i+1}), \end{cases} \tag{2.1}$$

where Ω is a number between 0 and 1 that fixes the location of the discontinuity between these two states. The initial data $U(x, t_j)$ is therefore piecewise constant; it equals either $U(x_i, t_j)$ or $U(x_{i+1}, t_j)$ depending on the particular location of the discontinuity between the two nodes.

With increasing time beyond t_j the discontinuity between the two initial states will break into leftward and rightward moving waves which are separated by a contact surface [1–11]. Each wave can be either a shock or a rarefaction wave depending on the initial data, and the available combinations produce four unique wave patterns which are self-similar (i.e., depend on x/t only). These patterns are

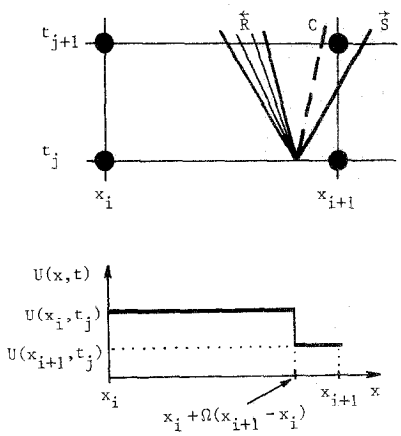

FIG. 1. Initial piecewise constant data $U(x, t)$ for a Riemann problem on a nonstaggered grid.

depicted in Fig. 2. It should be noted that a fifth wave pattern is also possible, and this pattern is the particular case when a vacuum exists between two contact surfaces, all of which occur between two rarefaction waves [3]. This is also shown in Fig. 2. Although this last case is of theoretical interest only [5, 24], because it is the limit of the perfect gas equations at zero pressure and temperature, it can never be realized in practice. Real-gas effects such as molecular vibration, particle covolume and gas liquifaction would violate the assumption of a perfect gas and also prevent such an ideal vacuum from developing in reality.

The problem of determining the types of waves, their strengths, and the flow properties in each region between the waves and contact surface for some particular set of initial data is called a Riemann problem, and the algorithm for determining

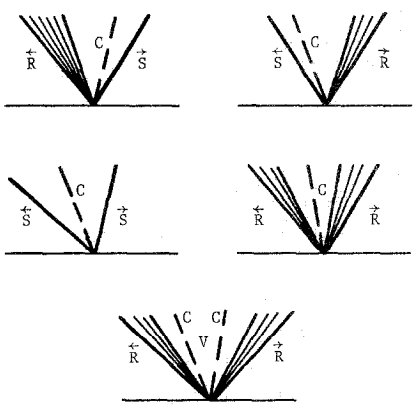

FIG. 2. Five possible wave patterns in the solution of a Riemann problem, showing shock (S) and rarefraction (R) waves separated by a contact surface (C). The last one has a vacuum (V) in the pattern center.

the solution to this problem is called a Riemann solver. For the one-dimensional unsteady Euler equations and a perfect gas the solution of the Riemann problem always exists, and it requires the determination of six state variables p_l^*, ρ_l^*, u_l^*, p_r^*, ρ_r^*, and u_r^* on the two sides of the contact surface. These unknowns can be obtained by using the three conservation laws of mass, momentum, and energy and the equation of state. These laws reduce to the well-known Rankine–Hugoniot relations across shocks [25] and to the well-known isentropic characteristic equations across rarefaction waves [25]. These nonlinear and algebraic equations may be used to jump across the leftward maving wave from the known left state (p_1, ρ_1, u_1) to the unknown state (p_l^*, ρ_l^*, u_l^*) to the left of the contact surface. The shock relations are employed if $p_l^* \geqslant p_1$, and the rarefaction-wave equations are used if $p_l^* < p_1$. Similarly, the shock and rarefaction-wave equations may be used to jump across the rightward moving wave from the known right state (p_r, ρ_r, u_r) to the unknown state (p_r^*, ρ_r^*, u_r^*) to the right of the contact surface. By employing $p^* = p_l^* = p_r^*$ and $u^* = u_l^* = u_r^*$ across the contact surface, the set of equations describing the Riemann problem may be reduced to a single nonlinear algebraic equation in one unknown for any particular wave pattern. However, this equation generally is implicit in the unknown p^* or u^* and an iterative solution scheme is required. Different iterative schemes or Riemann solvers will be introduced in the next section.

The manner in which Riemann problems are incorporated in various computational methods to solve a complete flow field varies greatly depending on whether the numerical integration scheme is based on finite differences, finite volumes, or random samplings. In the specific case of the random-choice method a random sampling that uses the quasirandom number of Van der Corput [26, 27] is employed to locate the discontinuity, and the wave pattern can be overlaid or mapped onto a time–distance diagram, as illustrated in Fig. 1. The solution of whatever part of the wave pattern that overlaps the left or right grid node at the next time level is then assigned directly to this node, as the approximate solution. For the case shown in Fig. 1, the state between the shock and contact surface is assigned to the right node at level t_{j+1}. The pattern can not simultaneously overlap both the left and right nodes because the Courant–Friedrichs–Lewy time step criteria will sufficiently limit the size of the time step. This explicit procedure may be repeated for all other cells on the same time level and cells on subsequent levels, in order to construct a complete flow-field solution. Additional details of the random sampling and assignment procedure for a nonstaggered grid with a variable node spacing and local time stepping have been given previously by Gottlieb [15].

Before presenting different Riemann solvers it is worthwhile examining the Riemann problem more closely. The solutions for different wave patterns may be illustrated conveniently on the classical pressure–velocity diagram for solving wave interaction problems [25, 28]. Let us begin with the states on the left and right sides of the initial discontinuity; they are known and will be denoted by $(p_1, a_1, u_1, \gamma_1, R_1)$ and $(p_r, a_r, u_r, \gamma_r, R_r)$. The left state is shown in the diagram of Fig. 3 as one point fixed by arbitrary values of p_1 and u_1. Let the right state be

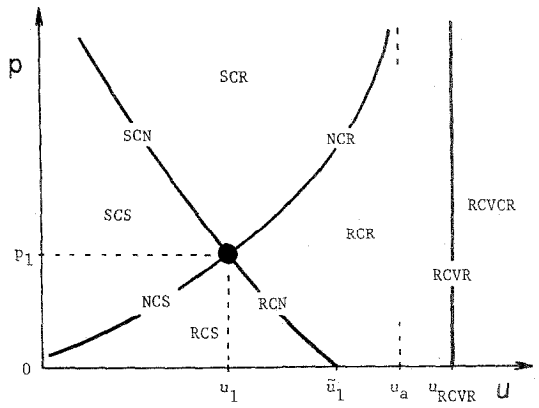

FIG. 3. Five wave pattern regions and boundaries in the pressure–Velocity diagram for the left state (p_1, u_1). Note that $\tilde{u}_1 = u_1 + 2a_1/(\gamma_1 - 1)$, $u_a = u_1 + 2a_r/(\gamma_r - 1)$, $u_{RCVR} = \tilde{u}_1 + 2a_r/(\gamma_r - 1)$.

anywhere else on this diagram. Five curved lines labeled *SCN*, *NCR*, *NCS*, *RCN*, and *RCVR* are the boundaries between the five regions labeled *SCS*, *SCR*, *RCR*, *RCS* and *RCVCR*, and each region corresponds to one of the wave patterns shown in Fig. 2. The notation should be fairly obvious; *RCS* denotes a wave pattern with a rarefaction wave moving to the left and a shock moving to the right, separated by contact surface. At each boundary one of the waves from the two adjacent patterns on either side of the boundary becomes nonexistent or simply degenerates to a Mach wave. Hence, *NCS* denotes a wave pattern with no wave or just a Mach wave travelling to the left and a shock travelling to the right, with a contact surface between these waves.

The five boundaries may be expressed analytically in closed form for arbitrary left and right states. Without derivation they are given as follows:

$$u_{SCN} = u_1 - \frac{a_1}{\gamma_1}\left[\frac{p_r}{p_1} - 1\right]\left[\frac{\gamma_1 + 1}{2\gamma_1}\frac{p_r}{p_1} + \frac{\gamma_1 - 1}{2\gamma_1}\right]^{-1/2} \quad \text{for} \quad p_r \geqslant p_1, \tag{2.2}$$

$$u_{NCS} = u_1 - \frac{a_r}{\gamma_r}\left[\frac{p_1}{p_r} - 1\right]\left[\frac{\gamma_r + 1}{2\gamma_r}\frac{p_1}{p_r} + \frac{\gamma_r - 1}{2\gamma_r}\right]^{-1/2} \quad \text{for} \quad p_r \leqslant p_1, \tag{2.3}$$

$$u_{NCR} = u_1 + \frac{2a_r}{\gamma_r - 1}\left[1 - \left[\frac{p_1}{p_r}\right]^{(\gamma_r - 1)/2\gamma_r}\right] \quad \text{for} \quad p_r \geqslant p_1, \tag{2.4}$$

$$u_{RCN} = u_1 + \frac{2a_1}{\gamma_1 - 1}\left[1 - \left[\frac{p_r}{p_1}\right]^{(\gamma_1 - 1)/2\gamma_1}\right] \quad \text{for} \quad p_r \leqslant p_1, \tag{2.5}$$

$$u_{RCVR} = u_1 + \frac{2}{\gamma_1 - 1}a_1 + \frac{2}{\gamma_r - 1}a_r \quad \text{for} \quad p_r \geqslant 0. \tag{2.6}$$

The *SCN* curve rises monotonically from p_1 and u_1 to $p = \infty$ at $u = -\infty$, whereas

the *NCS* curve falls continuously from p_1 and u_1 is asymptotic to $p=0$ as u decreases. The *RCN* curve decreases monotonically from p_1 and u_1 to $p=0$ at $\tilde{u}_1 = u_1 + 2a_1/(\gamma_1 - 1)$, whereas the *NCR* curve rises monotonically from p_1 and u_1 and is asymptotic to $u_a = u_1 + 2a_r/(\gamma_r - 1)$ as p increases. The *RCVR* line is vertical at the flow velocity u_{RCVR}, which is larger than u_a. Furthermore, the *SCN* and *RCN* boundaries, as well as the *NCS* and *NCR* boundaries, are not only matched in both pressure and velocity at their junction at the left state ($u_{SCN} = u_{RCN}$, $u_{NCS} = u_{NCR}$), but the first two derivatives dp/du and d^2p/du^2 are also matched there. Third and higher derivatives are not matched at this junction point because entropic changes are introduced by finite-amplitude shocks.

The equations for the boundaries help illustrate that a unique solution always exists for the Riemann problem for any arbitrary set of initial data defining the left and right states [3, 5, 6]. In other words, the solution is one of the five patterns shown in Fig. 2, and their five solution domains are distinct and also cover every part of the pressure–velocity diagram (without any overlap).

These boundary equations are also beneficial for determining the type of wave pattern without actually computing the solution of the Riemann problem by some iterative procedure. For example, let the pressure of the right state be higher than that of the left state ($p_r > p_1$). If u_r is less than u_{SCN} then the pattern must be *SCS*, if u_r lies between u_{NCR} and u_{RCVR} then the pattern is *SCR*, if u_r lies between u_{NCR} and u_{RCVR} then the pattern must be *RCR*, and so on and so forth. These equations may also be helpful in deriving an initial guess for the iterative procedure, and this will be illustrated in the next section.

Solutions to different Riemann problems are illustrated graphically in the pressure–velocity diagram of Fig. 4. An arbitrary left state is indicated by the solid circle and four right states for different wave patterns are shown as open circles. The solution for each pair of left and right states is given by the open triangle. Although in this diagram the solution corresponds to a common pressure p^* and common velocity u^* across the contact surface, the rest of the solution would also include other state properties such as ρ_1^* and ρ_r^*, and a_1^* and a_r^*.

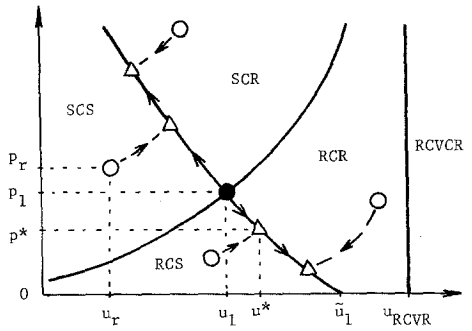

FIG. 4. Graphical illustration of solutions (△) for the left state (●) and various right states (○).

Before concluding this discussion of the Riemann problem, two additional interesting features should be mentioned. First, although the solution to most Riemann problems involves an iterative procedure, the problem which has a wave pattern featuring two rarefaction waves separated by a contact surface may be solved explicitly for p^* and u^*, provided that $\gamma_r = \gamma_1$ [3]. The particular solutions for p^* and u^* on either side of the contact surface are

$$p^* = p_1 \left[\frac{\gamma - 1}{2} \frac{\tilde{u}_1 - \tilde{u}_r}{a_1(1+z)} \right]^{2\gamma/(\gamma-1)}, \tag{2.7}$$

$$u^* = \frac{\tilde{u}_1 z + \tilde{u}_r}{1+z}, \tag{2.8}$$

where

$$\tilde{u}_1 = u_1 + \frac{2}{\gamma_1 - 1} a_1, \qquad \tilde{u}_r = u_r - \frac{2}{\gamma_r - 1} a_r, \tag{2.9}$$

$$z = \frac{a_r}{a_1} \left[\frac{p_1}{p_r} \right]^{(\gamma-1)/2\gamma}, \tag{2.10}$$

and $\gamma = \gamma_1 = \gamma_r$. This solution may be used as an approximate solution instead of an iterative procedure to reduce computational time and cost.

The second interesting feature of the Riemann problem is that the flow direction may be determined without computing the full solution by iteration. This can be accomplished rather simply by introducing an artificial stationary boundary or wall between the left and right states and calculating the pressures that would act on the left and right sides of this boundary. The flow direction will then be from the side with the higher pressure to the side with the lower pressure. If the flow at the left state is positive ($u_1 \geqslant 0$) a shock will be reflected from the left side of this boundary and the pressure p_L on this side will be dictated by $p_1[1 + \gamma_1(\gamma_1+1)\, M_1^2/4 + \gamma_1 M_1(1 + \{\gamma+1\}^2\, M_1^2/16)^{1/2}]$, where $M_1 = u_1/a_1$. On the other hand, if the flow is away from the left side of the boundary ($u_1 < 0$), a rarefaction wave will be reflected instead. Then p_L equals $p_1[1 + (\gamma_1 - 1)\, M_1/2]^{2\gamma_1/(\gamma_1-1)}$ if $\tilde{u}_1 > 0$, or $p_L = 0$ if $\tilde{u}_1 \leqslant 0$ (vacuum). The procedure may be repeated for the right side of the boundary. For a reflected shock ($u_r < 0$) we have $p_R = p_r[1 + \gamma_r(\gamma_r+1) M_r^2/4 - \gamma_r M_r(1 + \{\gamma_r+1\}^2\, M_r^2/16)^{1/2}]$ with $M_r = u_r/a_r$, and for a reflected rarefaction wave ($u_r > 0$) the equation is $p_r[1 - (\gamma_r - 1)\, M_r/2]^{2\gamma_r/(\gamma_r-1)}$ if $\tilde{u}_r < 0$, or $p_R = 0$ if $\tilde{u}_r \geqslant 0$ (vacuum). The fact that the flow is in the direction from the larger to the smaller pressure can be proved rigorously by using the pressure–velocity diagram. A vertical line is drawn at $u = 0$ and p_L and p_R are located on this line. The solution for p^* will lie between p_L and p_R. More importantly, u^* will be positive valued and lie on the right side of the vertical boundary at $u = 0$ whenever $p_L > p_R$, or u^* will be negative valued and lie on the left side of this line whenever $p_L < p_R$. This proves that the flow direction is always from the side of the boundary with the higher reflected pressure to that of the lower reflected pressure.

3. Riemann Solvers

A number of different exact Riemann solvers have been developed over the past thirty years because there are a variety of ways in which to express the shock and rarefaction-wave equations, and different solvers employ different iterative solution techniques with different initial guesses. These Riemann solvers are presented briefly without derivation in this section, but further details are available in the original references.

3.1. *Godunov's First Method*

In Godunov's early computational studies [1, 2] of unsteady one- and two-dimensional flows he introduced an elegant method of solving Riemann problems for polytropic gases, which was presented as an integral part of his first- and second-order finite-difference schemes for the Euler equations. Although some of the elegance of the combined difference schemes and Riemann solver are unfortunately lost when the solver is considered alone, this is unavoidable here. The equations representing his solver are summarized in the notation of this paper for the initial left and right states. Although Godunov did not generalize his results for different gases in the initial left and right state, this simple generalization is included herein.

The pressure p^* on each side of the contact surface is related implicitly to the mass fluxes passing through the left and right waves (A and B) by the expression

$$p^* = (Bp_l + Ap_r + AB\{u_l - u_r\})/(A + B), \tag{3.1}$$

where

$$A = \begin{cases} (\gamma_l \rho_l p_l)^{1/2} \left[\dfrac{\gamma_l + 1}{2\gamma_l} \dfrac{p^*}{p_l} + \dfrac{\gamma_l - 1}{2\gamma_l} \right]^{1/2} & \text{for } p^* \geqslant p_l, \\ \dfrac{\gamma_l - 1}{2\gamma_l} (\gamma_l \rho_l p_l)^{1/2} \dfrac{1 - p^*/p_l}{1 - (p^*/p_l)^{(\gamma_l - 1)/2\gamma_l}} & \text{for } p^* < p_l, \end{cases} \tag{3.2}$$

$$B = \begin{cases} (\gamma_r \rho_r p_r)^{1/2} \left[\dfrac{\gamma_r + 1}{2\gamma_r} \dfrac{p^*}{p_r} + \dfrac{\gamma_r - 1}{2\gamma_r} \right]^{1/2} & \text{for } p^* \geqslant p_r, \\ \dfrac{\gamma_r - 1}{2\gamma_r} (\gamma_r \rho_r p_r)^{1/2} \dfrac{1 - p^*/p_r}{1 - (p^*/p_r)^{(\gamma_r - 1)/2\gamma_r}} & \text{for } p^* < p_r. \end{cases} \tag{3.3}$$

The elegance of the variables A and B becomes apparent when the three conservation laws are expressed in Lagrangian form as a set of jump conditions across leftward and rightward moving shock and rarefaction waves. For example, the conservation laws become $A[u] + [p] = 0$, $A[\rho^{-1}] - [u] = 0$, and $A[E + u^2/2] + [pu] = 0$ for any left wave and $B[u] - [p] = 0$, $B[\rho^{-1}] + [u] = 0$, and $B[E + u^2/2] - [pu] = 0$ for any right wave, where E is the specific internal

energy and [ ] denotes the wave jump conditions. Hence, by using $A[u]+[p]=0$ and $B[u]-[p]=0$ across the left and right waves of a Riemann problem, and $[u]=0$ and $[p]=0$ across the contact surface, one may derive Eq. (3.1) for p^*, or a similar expression for u^*. The elegance is also apparent when one realizes that the velocities of left and right shock are given rather simply by $V_l=u_l-A/\rho_l$ and $V_r=u_r+B/\rho_r$.

Godunov obtained the solution for p^* from Eqs. (3.1) to (3.3) by employing a fixed-point iterative scheme in the form

$$p^*_{i+1}=f(p^*_i, A\{p^*_i\}, B\{p^*_i\}), \tag{3.4}$$

where the function f is defined by Eq. (3.1). Godunov did not specify a convergence criterion in his work; however, it is assumed that the iterative process was stopped when p^* ceased to change within some tolerance (or the corresponding values of A and B ceased to change).

In the case of strong rarefaction waves this iterative scheme may fail to convergence. In order to make the iterative procedure convergent in all cases Godunov modified Eq. (3.4) to the form

$$p^*_{i+1}=[\alpha_i p^*_i+f(p^*_i, A\{p^*_i\}, B\{p^*_i\})]/[\alpha_i+1]. \tag{3.5}$$

If $\gamma=\gamma_l=\gamma_r$, Godunov used an expression for the weighting factor α_i given by

$$\alpha_i=\frac{\gamma-1}{3\gamma}(1-Z_i)\,Z_i^{-(\gamma+1)/2\gamma}[1-Z_i^{(\gamma-1)/2\gamma}]^{-1}-1, \tag{3.6}$$

where $Z_i=f(p^*_i, A\{p^*_i\}, B\{p^*_i\})/(p_l+p_r)$. If α_i happens to be negative valued then α_i is reset to zero, because no modification is needed. If γ_l and γ_r are not equal, then another appropriate weighting factor would be required.

After the iteration has converged successfully and the final values of p^*, A, and B have been obtained, then u^* is given by the equation

$$u^*=(p_l-p_r+Au_l+Bu_r)/(A+B), \tag{3.7}$$

which is derived from the jump conditions in the same manner as Eq. (3.1) for p^*. Other state properties on each side of the contact surface may be calculated by using the Rankine–Hugoniot relations for shocks or the characteristic equations for rarefaction waves, as required.

An initial guess of p^* is required to start the iterative procedure. In the case when $\gamma=\gamma_l=\gamma_r$ the initial guess is given by [2]

$$p^*=\tfrac{1}{2}(p_l+p_r)+\tfrac{1}{2}k(u_l+u_r), \tag{3.8}$$

where $k=(\gamma\{p_l+p_r\}\{\rho_l+\rho_r\}/4)^{1/2}$. For the more general case when γ_l and γ_r are unequal, the intitial guess

$$p^*=\frac{\rho_l a_l p_r+\rho_r a_r p_l+\rho_l a_l \rho_r a_r(u_l-u_r)}{\rho_l a_l+\rho_r a_r} \tag{3.9}$$

is used [3]. Both guesses are based on weak wave or acoustic theory, and when shock and rarefaction waves become stronger these guesses become less accurate. However, it should be remembered that weak waves are prevalent in Riemann problems which are solved during computations of gasdynamic flow fields, and strong waves are encountered infrequently. Hence, these initial guesses are fairly accurate for the majority of Riemann problems.

When implementing Godunov's Riemann solver on digital computers the following precaution should be taken. The second expressions of Eqs. (3.2) and (3.3) for A and B across expansion waves are difficult to evaluate accurately on a digital computer when the pressure ratios p^*/p_r are very close to unity. In this case the expressions for A and B have finite values and are not theoretically singular; however, in practice computer roundoff errors may frequently result in very erroneous values computed for A and B. In Godunov's Riemann solver a special check and possible correction must be made during each iteration to overcome this problem.

3.2. *Godunov's Second Method*

Godunov developed a second Riemann solver which was computationally more efficient [3]. He expressed the shock and rarefaction-wave equations in a much simpler form, and this not only eliminates the difficulty in evaluating the rarefaction-wave expressions but simultaneously reduces the number of mathematical operations per iterative cycle. Furthermore, the problematic fixed-point iterative scheme was replaced by a higher order and trouble-free Newton method, in order to accelerate convergence and reduce computational efforts. In this second Riemann solver Godunov still retained the initial guess for p^* that was derived from acoustic theory.

In Godunov's second method a function $F(p^*)$ is defined as the difference between the flow velocities on the two sides of the contact surface; that is, $F(p^*) = u_r^*(p^*) - u_l^*(p^*)$. For the more general case of different gases in the initial left and right states, this function may be expressed as

$$F(p^*) = f(p^*, p_l, a_l, \gamma_l) + f(p^*, p_r, a_r, \gamma_r) - u_l + u_r, \tag{3.10}$$

where

$$f(p^*, p, a, \gamma) = \begin{cases} \dfrac{a}{\gamma}\left[\dfrac{p^*}{p} - 1\right]\left[\dfrac{\gamma+1}{2\gamma}\dfrac{p^*}{p} + \dfrac{\gamma-1}{2\gamma}\right]^{-1/2} & \text{for } p^* \geqslant p, \\ \dfrac{2a}{\gamma-1}\left[\left[\dfrac{p^*}{p}\right]^{(\gamma-1)/2\gamma} - 1\right] & \text{for } p^* < p. \end{cases} \tag{3.11}$$

Hence, the solution for p^* corresponds to the particular case when the function $F(p^*)$ is equal to zero.

The higher order Newton iterative scheme which makes use of the first and second derivatives of $F(p^*)$ may be expressed in the form [3]

$$p_{i+1}^* = p_i^* - \frac{F}{F'} - \frac{F^2 F''}{2(F')^3}, \tag{3.12}$$

where F denotes $F(p_i^*)$ for brevity and the prime designates differentiation with respect to p^*. (In this higher order method a tangent parabola instead of a tangent straight line is used to estimate the root.) The corresponding first and second derivatives of the function $f(p^*, p, a, \gamma)$ may be written as

$$f'(p^*, p, a, \gamma) = \begin{cases} \dfrac{(\gamma+1)\,a}{4\gamma^2 p}\left[\dfrac{p^*}{p} - \dfrac{3\gamma-1}{\gamma+1}\right]\left[\dfrac{\gamma+1}{2\gamma}\dfrac{p^*}{p} + \dfrac{\gamma-1}{2\gamma}\right]^{-3/2} & \text{if } p^* \geqslant p, \\ \dfrac{a}{\gamma p^*}\left[\dfrac{p^*}{p}\right]^{(\gamma-1)/2\gamma} & \text{if } p^* < p, \end{cases} \tag{3.13}$$

and

$$f''(p^*, p, a, \gamma) = \begin{cases} -\dfrac{(\gamma+1)^2 a}{16\gamma^3 p^2}\left[\dfrac{p^*}{p} + \dfrac{7\gamma-1}{\gamma+1}\right]\left[\dfrac{\gamma+1}{2\gamma}\dfrac{p^*}{p} + \dfrac{\gamma-1}{2\gamma}\right]^{-5/2} & \text{if } p^* \geqslant p, \\ -\dfrac{(\gamma+1)a}{2(\gamma p^*)^2}\left[\dfrac{p^*}{p}\right]^{(\gamma-1)/2\gamma} & \text{if } p^* < p, \end{cases} \tag{3.14}$$

without difficulty.

To initiate the iterative procedure Godunov used the initial guess given earlier by Eq. (3.9). He noted that this initial guess will cause the iteration to approach the root in a well-behaved manner from below if $p_1 < p_r$, such that all p_i^* values in the iterative process are positive valued. In the other case when $p_1 > p_r$ one must perform a check for a negative valued p_i^*. If this occurs then p_i^* may be reset equal to $0.01 p_{i-1}^*$.

It is worth mentioning that Zhang and Gottlieb [20] developed a very similar Riemann solver which employed a Newton iterative method, without prior knowledge of Godunov's second method [3]. In their study, Zhang and Gottlieb investigated the relative computatioal savings that could be achieved by using Newton's method with first and second derivatives. Their findings suggest that the faster convergence rate (reduced number of iterations) of Newton's method with second derivatives was offset by the increased number of mathematical operations to compute the higher derivatives, except in the cases when the left and right waves of the Riemann problem are fairly strong or the initial guess is inaccurate. Their study points out that nothing practical is gained by using the higher order Newton method when the standard Newton technique will provide equivalent or better computational performance.

3.3. *Chorin's Iterative Scheme*

Chorin [9] adopted to a large degree the first Riemann solver of Godunov with the same fixed-point iterative scheme, but he made some notable changes to the iterative solution procedure, and the combination of these modifications improved the overall efficiency substantially. Since the equations employed by Chorin are essentially the same as those used by Godunov, they are not repeated here. Only Chorin's modifications are discussed.

Chorin's first change involved the initial guess p^*. Instead of using the acoustic approximation given by Eq. (3.8) or (3.9), he used the average pressure $(p_l + p_r)/2$ and claimed that Godunov's initial guess was ineffective and that his initial guess gave better results. Chorin's claim is generally incorrect. In the case of strong waves both of their initial guesses are relatively ineffective; however, in the opposite case of weak waves, which occur frequently in Riemann problems of gasdynamics, Godunov's guess is definitely superior. Another disadvantage of Chorin's simpler initial guess is that the iterative procedure must be completed at least twice to avoid a spurious convergence when the initial pressures p_l and p_r are equal.

Another change introduced by Chorin involved the resolution of negative values of p_i^* which sometimes occur during the iterative process. Chorin circumvented the occurrence of negative iterates by imposing a minimum allowable value for p_i^*, typically a very small positive number (10^{-6}). Chorin also modified the determination of convergence. He chose to terminate the iterative process when changes in successive values of both A and B became smaller than some small tolerance (e.g., 10^{-6}). This imposes two separate checks on A and B instead of only one for p_i^*.

Finally, Chorin's most important modification to Godunov's first method to improve the computational efficiency of the fixed-point iterative scheme involved circumventing convergence failure in the presence of a strong rarefaction wave. Instead of adopting Godunov's cumbersome and computationally inefficient method of making the iterative process convergent for all possible cases by adding Eqs. (3.5) and (3.6), Chorin devised a relatively simple alternate procedure. If the iterative procedure does not converge after 20 iterations Chorin suggests computing the next iterate by using

$$p_{i+1}^* = \alpha \max(\varepsilon, p_i^*) + (1-\alpha)p_i^* \tag{3.15}$$

with $\varepsilon = 10^{-6}$ and $\alpha = \frac{1}{2}$. If a further 20 iterations do not give convergence, then Eq. (3.15) is used once again, but this time with $\alpha = \frac{1}{4}$, and so on and so forth. Chorin's procedure reduces the costly overhead of computing Godunov's cumbersome expressions (Eqs. (3.5) and (3.6)) for each iterative cycle, whether they are required or not, and this greatly reduces the computational effort.

3.4 *Van Leer's Iterative Scheme*

Van Leer [29] adopted the form of the shock and rarefaction-wave equations used in Godunov's first method. However, he and a colleague P. J. Bedijn

abandoned the trouble-some and inefficient fixed-point iterative procedure in favor of the standard Newton method, in order to improve the convergence rate. Furthermore, Van Leer showed that the implementation of Newton's method with the first derivatives of the shock and rarefaction-wave equations was not very difficult and produced valuable reductions in computational effort .

Van Leer chose to iterate with the pressure of the states on each side of the contact surface (p^*) and make the flow velocity difference $u_l^* - u_r^*$ equal to zero, as Godunov did in his second Riemann solver. Hence, new values of p^* may be obtained by using Newton's method in the form

$$p_{i+1}^* = p_i^* - \frac{u_l^*(p_i^*) - u_r^*(p_i^*)}{u_l^{*\prime}(p_i^*) - u_r^{*\prime}(p_i^*)}, \tag{3.16}$$

where

$$u_l^*(p^*) = u_l - \frac{p^* - p_l}{A(p^*, p_l, \gamma_l)}, \tag{3.17}$$

$$u_r^*(p^*) = u_r + \frac{p^* - p_r}{B(p^*, p_r, \gamma_r)}. \tag{3.18}$$

The expressions for u_l^* and u_r^* are derived from the wave jump conditions, and the functions A and B are defined previously by Eqs. (3.2) and (3.3). The first derivatives of u_l^* and u_r^* with respect to p^* are

$$u_l^{*\prime}(p^*) = \begin{cases} -(A^2 + C_l^2)/(2A^3) & \text{for } p^* \geqslant p_l, \\ -C_l^{-1}\left[\dfrac{p^*}{p}\right]^{-(\gamma_l+1)/2\gamma_l} & \text{for } p^* < p_l, \end{cases} \tag{3.19}$$

$$u_r^{*\prime}(p^*) \begin{cases} (B^2 + C_r^2)/(2B^3) & \text{for } p^* \geqslant p_r, \\ C_r^{-1}\left[\dfrac{p^*}{p}\right]^{-(\gamma_r+1)/2\gamma_r} & \text{for } p^* < p_r, \end{cases} \tag{3.20}$$

where $C_l = (\gamma_l p_l \rho_l)^{1/2}$ and $C_r = (\gamma_r p_r \rho_r)^{1/2}$. In the iterative procedure Van Leer used the initial guess of Godunov (Eq. (3.9)) and stopped the convergence when successive values of the iterate differed by some very small tolerance. If a negative iterate was encountered it was reset to a small positive number. Note that Van Leer's scheme and Godunov's second method are virtually the same, except that Van Leer has expressed his equations in a slightly shorter form.

3.5. *Smoller's Method*

Smoller's approach [6] in presenting the equations which apply across shocks, contact surfaces, and rarefaction waves of the Riemann problem is nonstandard but

highly elegant mathematically. For the leftward moving wave in the Riemann problem his equations are written as

$$\frac{p_1^*}{p_1} = \exp(-x), \tag{3.21}$$

$$\frac{\rho_1^*}{\rho_1} = f_1(x) = \begin{cases} \dfrac{\beta + \exp(x)}{1 + \beta \exp(x)} & \text{if } x \leqslant 0, \\ \exp(-x/\gamma) & \text{if } x > 0, \end{cases} \tag{3.22}$$

$$\frac{u_1^* - u_1}{a_1} = h_1(x) = \begin{cases} \dfrac{2\tau^{1/2}}{\gamma - 1} \dfrac{1 - \exp(-x)}{[1 + \beta \exp(-x)]^{1/2}} & \text{if } x \leqslant 0, \\ \dfrac{2}{\gamma - 1}[1 - \exp(-\tau x)] & \text{if } x > 0, \end{cases} \tag{3.23}$$

where $\beta = (\gamma + 1)/(\gamma - 1)$ and $\tau = (\gamma - 1)/2\gamma$. Note that the case of a shock corresponds to $x \leqslant 0$ and a rarefaction wave to $x > 0$. Also, these expressions have not been generalized for the case of different gases in the left and right states.

Across the contact surface Smoller defines the density ratio as

$$\rho_r^*/\rho_1^* = \exp(y) \tag{3.24}$$

and sets $p_1^* = p_r^*$ and $u_1^* = u_r^*$.

For the rightward moving wave in the Riemann problem Smoller's equations are written as

$$\frac{p_r}{p_r^*} = \exp(z), \tag{3.25}$$

$$\frac{\rho_r}{\rho_r^*} = f_r(z) = \frac{1}{f_1(z)}, \tag{3.26}$$

$$\frac{u_r - u_r^*}{a_r^*} = h_r(z) = \begin{cases} \dfrac{2\tau^{1/2}}{\gamma - 1} \dfrac{\exp(z) - 1}{[1 + \beta \exp(z)]^{1/2}} & \text{if } z \leqslant 0, \\ \dfrac{2}{\gamma - 1}[\exp(\tau z) - 1] & \text{if } z > 0. \end{cases} \tag{3.27}$$

In obtaining the solution to the Riemann problem Smoller combined his previous equations to give the intermediate results:

$$\frac{\rho_r}{\rho_1} = A = f_1(x) \exp(y) f_r(z), \tag{3.28}$$

$$\frac{p_r}{p_1} = B = \exp(z - x), \tag{3.29}$$

$$\frac{u_r - u_1}{a_1} = C = h_1(x) + h_r(z)[f_1(x) \exp(x + z)]^{-1/2}. \tag{3.30}$$

These equations may be manipulated into the final form [6]

$$h_1(x) + (B/A)^{1/2}\, h_1(x + \ln\{B\}) = C, \tag{3.31}$$

which provides an implicit expression for x. The variable x may be determined by an iterative procedure, and then z is obtained from Eq. (3.29) and y follows from Eq. (3.28). Once x, y, and z have been determined, the remainder of the flow properties on each side of the contact surface are computed easily by means of Eqs. (3.21) to (3.27). Note that a unique solution will always exist if the condition $2 + 2(B/A)^{1/2} > (\gamma - 1)\, C$ is satisfied, which is just the normal check to ensure that a vacuum state does not exist at the contact surface.

Smoller's equations representing the Riemann problem were employed in a Riemann solver developed by Dutt [30]. Dutt solved the equations by using the regula-falsi iterative scheme (false position), which is a combination of the well-known bisection technique with a secant method. This scheme has a slower rate of convergence rate than Newton's method. Dutt employed a simple guess of $x = 0$ to start the iterative procedure. Note that Dutt's computer program was reconstructed from the listing given in his report, but it was modified slightly by implementing the proper check for the determination of convergence, in order to avoid arbitrarily large numbers of iterations in certain cases.

3.6. *A New Riemann Solver*

The most efficient Riemann solver will always be the one with the fewest number of mathematical operations for the entire solution procedure, which will include the initial guess, equations used in the iterative procedure, check to stop the iterative process, and additional expressions required to completely specify the states on both sides of the contact surface, as well as determine both the left and right wave speeds. In an attempt to develop a more efficient Riemann solver we have strived to employ the fewest and simplest equations possible to represent the Riemann problem, and we have used the standard Newton iterative method in conjuction with a new efficient initial guess. Another important feature of this new Riemann solver is the choice of state variables. From experience we have found that numerical computations of unsteady flows of inviscid and perfect gases are slightly more efficient when the states at grid nodes are defined by (p, a, u, γ, R) instead of (p, ρ, u, γ, R), because the speed of sound is dependent variable which appears more frequently than the density in the equations. For example, it occurs directly in the characteristic equations for rarefaction waves, in computing shock and expansion wave speeds, and in the calculations of the Courant–Friedrichs–Lewy time step. It easily replaces the density in the Rankine–Hugoniot relations for shock waves. The sound speed is used to advantage as one of the dependent variables in this new Riemann solver.

Instead of solving for the common pressure of the intermediate states (p^*), the common flow velocity of the intermediate states (u^*) is used as the iterate in the new Riemann solver, and the pressure difference $p_l^* - p_r^*$ across this contact

discontinuity is made equal to zero. This is in direct contrast to all previous Riemann solvers (which iterate with p^*). However, this new approach helps improve the computational performance.

By using the standard Newton iterative procedure to determine the solution of the Riemann problem, successive iterates of u^* are given by

$$u_{i+1}^* = u_i^* - \frac{p_l^*(u_i^*) - p_r^*(u_i^*)}{p_l^{*\prime}(u_i^*) - p_r^{*\prime}(u_i^*)}, \tag{3.32}$$

where the prime denotes differentiation with respect to u^*. In this solution process, convergence is determined by satisfying the inequality $|1 - p_l^*/p_r^*| < \varepsilon$, and the tolerance ε is usually 10^{-6}. The other shock and rarefaction equations that yield p_l^*, p_r^*, a_l^*, a_r^*, dp_l^*/du^*, and dp_r^*/du^* follow without derivation.

In the case of the leftward moving shock of the Riemann problem, for which $u^* \leqslant u_l$, the pertinent equations are

$$W_l = \frac{\gamma_l + 1}{4}\frac{u^* - u_l}{a_l} - \left[1 + \left[\frac{\gamma_l + 1}{4}\frac{u^* - u_l}{a_l}\right]^2\right]^{1/2}, \tag{3.33}$$

$$p_l^* = p_l + C_l(u^* - u_l)\, W_l, \tag{3.34}$$

$$p_l^{*\prime} = \frac{2C_l W_l^3}{1 + W_l^2}, \tag{3.35}$$

$$a_l^* = a_l \left[\frac{(\gamma_l + 1) + (\gamma_l - 1)\, p_l^*/p_l}{(\gamma_l + 1) + (\gamma_l - 1)\, p_l/p_l^*}\right]^{1/2}, \tag{3.36}$$

where $C_l = \gamma_l p_l/a_l$ is computed before the iterative procedure begins, and W_l is the shock Mach number with respect to the moving gas ahead of the shock. W_l is a by-product of the iteration. Note that the shock velocity V_l is given by $u_l + a_l W_l$ in the laboratory reference frame. Also, the variables a_l^* and V_l are not needed in the iterative procedure and should therefore be computed later.

For a rightward moving shock for which $u^* \geqslant u_r$ the equations are

$$W_r = \frac{\gamma_r + 1}{4}\frac{u^* - u_r}{a_r} + \left[1 + \left[\frac{\gamma_r + 1}{4}\frac{u^* - u_r}{a_r}\right]^2\right]^{1/2}, \tag{3.37}$$

$$p_r^* = p_r + C_r(u^* - u_r)\, W_r, \tag{3.38}$$

$$p_r^{*\prime} = \frac{2C_r W_r^3}{1 + W_r^2}, \tag{3.39}$$

$$a_r^* = a_r \left[\frac{(\gamma_r + 1) + (\gamma_r - 1)\, p_r^*/p_r}{(\gamma_r + 1) + (\gamma_r - 1)\, p_r/p_r^*}\right]^{1/2}, \tag{3.40}$$

where $C_r = \gamma_r p_r/a_r$ and W_r is the shock Mach number. Again, the shock velocity V_r

is given by $u_r + a_r W_r$ in the laboratory frame of reference, and the variables V_r and a_r^* are not required in the iterative process and should therefore be computed afterwards.

For a left rarefaction wave with $u^* > u_1$ the relevant equations are

$$a_1^* = a_1 - \frac{\gamma_1 - 1}{2}(u^* - u_1), \tag{3.41}$$

$$p_1^* = p_1 \left[\frac{a_1^*}{a_1}\right]^{2\gamma_1/(\gamma_1 - 1)}, \tag{3.42}$$

$$p_1^{*\prime} = -\gamma_1 p_1^*/a_1^*. \tag{3.43}$$

In this case a_1^* is a by-product of the iterative procedure, and the velocity of rarefaction-wave head $u_1 - a_1$ and tail $u_1^* - a_1^*$ in the laboratory frame of reference should be computed after the iterative process is completed.

In the other case of the right rarefaction wave the equations are

$$a_r^* = a_r + \frac{\gamma_r - 1}{2}(u^* - u_r), \tag{3.44}$$

$$p_r^* = p_r \left[\frac{a_r^*}{a_r}\right]^{2\gamma_r/(\gamma_r - 1)}, \tag{3.45}$$

$$p_r^{*\prime} = \gamma_r p_r^*/a_r^*. \tag{3.46}$$

In this case a_r^* is a by-product of the iterative process, and the velocity of expansion-wave head $u_r + a_r$ and tail $u_r^* + a_r^*$ in the laboratory frame of reference may be computed after the iteration is completed.

To start the solution procedure the initial guess for the flow velocity u_0^* is obtained by using the expressions

$$u_0^* = \frac{\tilde{u}_1 z + \tilde{u}_r}{1 + z}, \tag{3.47}$$

where

$$\tilde{u}_1 = u_1 + \frac{2}{\gamma_1 - 1} a_1, \qquad \tilde{u}_r = u_r - \frac{2}{\gamma_r - 1} a_r, \tag{3.48}$$

$$z = \frac{\gamma_1 - 1}{\gamma_r - 1}\frac{a_r}{a_1}\left[\frac{p_1}{p_r}\right]^{(\sigma - 1)/2\sigma} \quad \text{with} \quad \sigma = \begin{cases} \gamma_1 & \text{if } p_1 \geqslant p_r, \\ \gamma_r & \text{if } p_1 < p_r. \end{cases} \tag{3.49}$$

On the other hand, the initial guess p_0^* can be expressed in the form

$$p_0^* = p_1 \left[\frac{\gamma_1 - 1}{2}\frac{\tilde{u}_1 - \tilde{u}_r}{(1 + z)\, a_1}\right]^{2\gamma_1/(\gamma_1 - 1)}, \tag{3.50}$$

which is more cumbersome because of the extra power. These initial guesses have a graphical interpretation on the pressure–velocity diagram. Consider the case when $p_1 < p_r$ first, for which the right state is higher in the diagram than the left state and

also located in the *RCR* domain as indicated in Fig. 5. One can see that the right state for a *RCR* wave pattern must have a velocity u_r which lies between boundary values u_{NCR} and u_{RCVR} at the pressure level of p_r, whereas the actual solution u^* must be in the range from u_1 to $\tilde{u}_1$. If it is assumed that the initial guess u^* lies in the same proportion between u_1 and $\tilde{u}_1$ as u_r lies between U_{NCR} and u_{RCVR}, this guess is then given by $u_0^* = u_1 + (u_r - u_{NCR})(\tilde{u}_1 - u_1)/(u_{RCVR} - u_{NCR})$. This expression may be reduced to those given earlier by Eqs. (3.47) to (3.49). In the other case in which $p_1 > p_r$ we note that u_r now lies between u_{RCN} and u_{RCVR} for a *RCR* pattern By using the same method of proportions the other initial guess is similarly determined from $u_0^* = u_{RCN} + (u_r - u_{RCN})(\tilde{u}_1 - u_{RCN})/(u_{RCVR} - u_{RCN})$, and it also reduces to Eqs. (3.47) to (3.49).

Although these results for the initial guess may appear to be restricted to the *RCR* wave pattern domain only, this is untrue. The initial guess may be extrapolated beyond the *RCR* domain into the other *SCR*, *RCS*, and *SCS* domains. However, in general, the intitial guess becomes less accurate as the right state moves farther to the left of the *NCR* and *RCN* boundaries and one or both shocks in the wave patterns become stronger.

Some interesting aspects of this initial guess are worth mentioning. In the particular case when $\gamma = \gamma_1 = \gamma_r$, which will occur frequently in unsteady flow computations, the initial guess is the exact solution for u^* for the case of the *RCR* wave pattern. Equations (3.47) to (3.49) reduce to those given earlier by Eqs. (2.8) to (2.10). Hence, if $\gamma_1 = \gamma_r$, a simple check to determine if u_0^* lies between u_1 and u_r will immediately indicate whether the wave pattern is *RCR* and u_0^* is part of the exact solution. If this is the case, the complete solution should then be determined directly, to bypass the Newton iterative procedure and save some computational effort (about 4 to 7%).

Another interesting feature is that the intitial guess is the exact solution for the case of $\gamma_1 = \gamma_r$ and isentropic left and right waves, that is, if the shocks in the Riemann problem were replaced by compression waves. This is true even if the left

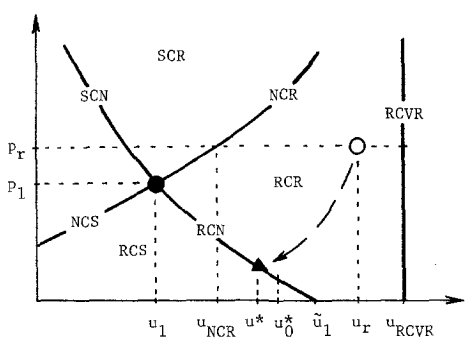

FIG. 5. Illustration of determining the initial guess u_0^*. For a right state (0) in the *RCR* domain u_r lies between u_{NCR} and u_{RCVR}, and the solution u_0^* lies between u_1 and $\tilde{u}_1$ in the same proportion.

and right states have different entropies. Hence, this initial guess will be very accurate for wave patterns with shocks which have small entropy changes (e.g., pressure ratios less than about 2), and it will be much superior to any initial guess based on acoustic theory. Furthermore, in most cases this new initial guess will still provide good estimates for much higher pressure ratios than 2. For example, if two flows with similar pressures and sound speeds in the left and right states collide and produce an *SCS* pattern in which the shocks are strong, the initial guess u_0^* would be accurate with a velocity near zero, and it would in turn predict fairly accurate values of p_l^* and p_r^*. It should be noted that if this isentropic wave theory was used to predict p_0^* instead of u_0^*, it would be inaccurate for strong shocks and the resulting values for u_l^* and u_r^* would be correspondingly inaccurate. This is a good illustration of one additional advantage of iterating with u^* instead of with p^* as in previous Riemann solvers.

In the other case when γ_l and γ_r are unequal, the new initial guess is exact only at the boundaries *NCR*, *RCN*, and *RCVR*. Elsewhere in the *RCR* domain and other *SCR*, *RCS*, and *SCS* domains it is simply approximate but still fairly accurate. It sould be remembered that Riemann problems with different gases in the left and right states occur infrequently in numerical computations.

Other initial guesses may also be developed by following this method of proportions. For example, for the *SCR* and *SCS* domains for which $p_l < p_r$, the initial guess may be expressed as $u_0^* = u_{SCN} + (u_r - u_{SCN})(\tilde{u}_l - u_{SCN})/(u_{NCR} - u_{SCN})$. However, such guesses are normally more harmful than helpful because they add computational overhead almost equivalent to completing a full iterative cycle, and most often the guess is not sufficiently more accurate than the isentropic guess in reducing the number of iterations.

4. Performance of Riemann Solvers

The performance of various exact Riemann solvers given in the previous chapter is assessed in the following manner. All of the Riemann solvers were programmed on a digital computer. Forty Riemann problems were posed such that ten problems corresponded to each of the *SCS*, *SCR*, *RCR*, and *RCS* wave patterns. Furthermore, in each set of ten Riemann problems, two consisted of one or more strong waves and the other eight contained only weak waves. The computer program overhead was kept constant and small for each performance run, so that the separate Riemann solver subroutines could be assessed fairly.

The solution to each Riemann problem consisted of computing the common pressure p^* and flow velocity u^* on each side of the contact surface, and one additional variable for the left (ρ_l^* or a_l^*) and right (ρ_r^* or a_r^*) sides of the contact surface, in order to complete the minimum three state variables needed to specify these intermediate states. If the left wave was a shock then its velocity $u_l + a_l W_l$ in the laboratory frame of reference was also computed. This was also done for any right shock wave. If the left wave was an expansion wave then the velocity of both

the head $u_1 - a_1$ and tail $u_1^* - a_1^*$ were also calculated. This was similarly done for a right rarefaction wave. Finally, an attempt was made to ensure that the convergence criteria were equivalent for each Riemann solver, such that the solutions were computed to the same accuracy.

The various central processor unit (CPU) times required for each Riemann solver to compute solutions to the forty Riemann problems are summarized in Table I, normalized to the time of the fastest Riemann solver. Additional CPU times for most of the Riemann solvers are also given for the case when their initial guess was replaced by the new initial guess described in this paper. Note that these relative CPU times should be considered typical rather than exact, because they are problem dependent and forty problems cannot be considered as comprehensive.

The new Riemann solver has the best performance because it is made very efficient in terms of minimizing the number of mathematical operations to complete the entire solution process, from the new initial guess to the final computations of the wave speeds. The new initial guesses u_0^* and p_0^* are also helpful in reducing CPU times. When p_0^* is employed in other Riemann solvers it significantly reduces their CPU times by 25 to 40%, as can be seen in Table I.

Smoller's method [6] of presenting the equations for the Riemann solver used in Dutt's numerical solution procedure [30] perform badly in comparison to all the other methods. This can be attributed directly to the addition of numerous mathematically elegant but needless exponentials to the shock and rarefaction-wave expressions and partly to the slow convergence rate of the regula-falsi method. Godunov's first method [1, 2] and his modified method by Chorin [9] do not perform very well. This is mainly because the shock and expansion-wave equations are somewhat cumbersome, the initial guesses are not very accurate, and the

TABLE I

Relative Performance of Riemann Solvers

Type of Riemann solver	Relative time	Time with the new initial guess p_0^*
Godunov's first method	7.22	4.78
Godunov's second scheme with a normal Newton method	2.16	1.48
Godunov's second scheme with a higher order Newton method	2.17	1.62
Chorin's method	4.42	2.65
Von Leer's scheme	1.96	1.36
Smoller's scheme with Dutt's iterative procedure	24.7	
New iterative solution procedure with the new initial guess	1.00	

iterative procedure is a fixed-point scheme with a slow convergence rate. Chorin's method is faster than Godonov's by a factor of about two because he replaced Godunov's cumbersome modification for making the method convergent in all cases with a simpler and more efficient procedure.

Godunov's second method [3] and Van Leer's scheme [29] both have good and similar performance ratings. This might have been expected because they are virtually identical methods with similar efficiencies. Both employ fairly simple and very similar shock and rarefaction-wave equations, and both use the same initial guess and Newton's iterative solution process. Van Leer's method is slightly faster than Godunov's—by about 10%—because the derivatives in his Newton iterative method are expressed in a simpler form.

It is worth noting that Godunov's second method [3] with the standard Newton iterative scheme (first derivatives only) is just as efficient as the same method with the higher order Newton scheme (including second derivatives), when the acoustic guess of Godunov is used. On the other hand, when the new initial guess is included along with the higher order Newton scheme, Godunov's second method becomes less efficient. This shows that the higher order iterative scheme increases the number of mathematical operations for the entire convergence procedure, despite the reduction in the number of iterations to obtain convergence. A similar observation has been noted by Zhang and Gottlieb [20].

5. Concluding Remarks

From a historical viewpoint it should be mentioned that Godunov's first Riemann solver was available in scientific papers in Russian and in various translations to researchers outside the Soviet Union [1, 2]. As a consequence his method in modified form due to Chorin [9] has been used rather extensively (e.g., [9–11, 13–14, 16–19]). On the other hand, Godunov's second method [3] was not readily available because it was in a Russian book on numerical solutions to multidimensional problems in gasdynamics which was not readily available outside the Soviet Union. If this Riemann solver had been known it would have been the obvious choice for the numerical work by Chorin and his followers. However, in spite of its unavailability, it was eventually re-invented by Van Leer [29] and others [20] as a means of improving the performance of computer codes for solving unsteady gasdynamic problems. These improvements in Riemann solvers have now led to a new and more efficient solver.

Approximate, instead of exact, Riemann solvers which are based on linear or acoustic theory were often employed in the past Russian literature to reduce computational effort [1–3, 31]. However, the use of substantially faster computers today along with the new Riemann solver given in this study will make the use of approximate Riemann solvers unnecessary in many cases. In those cases where approximate Riemann solvers are still required and $\gamma_l = \gamma_r$, however, the acoustic approximations for p^* and u^* should possibly be abandoned in favor of the

substantially more accurate expressions given by Eqs. (3.47) and (3.50), which are based on isentropic wave theory.

ACKNOWLEDGMENTS

The assitance of D. S. Anderson in computer programming the Riemann problems is gratefully acknowledged. The contract funding from the Defence Research Establishment Valcartier and grants from the Natural Sciences and Engineering Research Council, both of Canada, are acknowledged with thanks.

REFERENCES

1. S. K. GODUNOV, *Mat. Sb.* **47**, 271 (1959).
2. S. K. GODUNOV, A. W. ZABRODYN, AND G. P. PROKOPOV, *U.S.S.R. Comput. Math. and Math. Phys.* **1** No. 6, 1187 (1961).
3. S. K. GODUNOV (Ed.), *Numerical Solution of Multidimensional Problems in Gasdynamics* (Nauka, Moscow, 1976), Chap. 2.
4. J. GLIMM, *Commun. Pure Appl. Math.* **18**, 697 (1965).
5. R. G. SMITH, *Trans. Amer. Math. Soc.* **249**, No. 1, 1 (1979).
6. J. SMOLLER, *Shock Waves and Reaction-Diffusion Equations* (Springer-Verlag, New York, 1983), p. 307.
7. T.-P. LIU, *J. Differential Equations* **18**, 218 (1975).
8. C. MOLER AND H. SMOLLER, *Arch. Rat. Mech. Anal.* **37**, 309 (1970).
9. A. J. CHORIN, *J. Comput. Phys.* **22**, 517 (1976).
10. A. J. CHORIN, *J. Comput. Phys.* **25**, 253 (1977).
11. G. A. SOD, *J. Fluid Mech.* **83**, 785 (1977).
12. P. L. ROE, *J. Comput. Phys.* **43**, 357 (1981).
13. P. COLELLA, *SIAM J. Sci. Stat. Comput.* **3**, 76 (1982).
14. P. COLELLA AND H. M. GLAZ, Lawrence Berkeley Laboratory Report LBL-15776, University of California, November 1983 (unpublished).
15. J. J. GOTTLIEB, *J. Comput. Phys.*, in press.
16. G. A. SOD, *J. Comput. Phys.* **27**, 1 (1978).
17. T. SAITO AND I. I. GLASS, *Prog. Aerospace Sci.* **21**, 201 (1984).
18. J. J. GOTTLIEB AND O. IGRA, *J. Fluid Mech.* **137**, 285 (1983).
19. O. IGRA AND J. J. GOTTLIEB, *AIAA J.* **23**, 1014 (1985).
20. K. Y. ZHANG AND J. J. GOTTLIEB, UTIAS Report 304, University of Toronto, 1986 (unpublished).
21. K.-M. LI AND M. HOLT, *Phys. Fluids* **24**, No. 5, 816 (1981).
22. J. FLORES AND M. HOLT, *J. Comput. Phys.* **44**, 337 (1981).
23. P. CONCUS AND W. PROSKUROWSKI, *J. Comput, Phys.* **30**, 153 (1979).
24. T.-P. LIU AND J. A. SMOLLER, *Adv. Appl. Math.* **1**, 345, (1980).
25. R. COURANT AND K. O. FRIEDRICHS, *Supersonic Flow and Shock Waves*, 5th ed. (Interscience, New York, 1967), pp. 172.
26. J. M. HAMMERSLEY AND D. C. HANDSCOMB, *Monte Carlo Methods* (Methuen, London, 1975), Chaps. 2–3.
27. VAN DER CORPUT, *Proc. K. Akad. Wet.* **38**, 813, 1058 (1935).
28. A. K. OPPENHEIM, P. A. URTIEW, AND A. J. LADERMAN, *Arch. Mech. Eng.* **11** (3), 441, (1964).
29. B. VAN LEER, *J. Comput. Phys.* **32**, 101, (1979).
30. P. DUTT, NASA Contractor Report 178042, Langley Research Center, 1986 (unpublished).
31. V. V. PODLUBNYI AND A. S. FONAREV, *Izv. Akad. Nauk SSSR Mekh. Zhidk. Gaza* **6**, 66, (1974).